



A Journal of the Gesellschaft Deutscher Chemiker

# Angewandte Chemie

GDCh

International Edition

[www.angewandte.org](http://www.angewandte.org)

## Accepted Article

**Title:** Chiral Self-Discrimination and Guest Recognition in Helicene-based Coordination Cages

**Authors:** Thorben R. Schulte, Julian J Holstein, and Guido H. Clever

This manuscript has been accepted after peer review and appears as an Accepted Article online prior to editing, proofing, and formal publication of the final Version of Record (VoR). This work is currently citable by using the Digital Object Identifier (DOI) given below. The VoR will be published online in Early View as soon as possible and may be different to this Accepted Article as a result of editing. Readers should obtain the VoR from the journal website shown below when it is published to ensure accuracy of information. The authors are responsible for the content of this Accepted Article.

**To be cited as:** *Angew. Chem. Int. Ed.* 10.1002/anie.201812926  
*Angew. Chem.* 10.1002/ange.201812926

**Link to VoR:** <http://dx.doi.org/10.1002/anie.201812926>  
<http://dx.doi.org/10.1002/ange.201812926>

## COMMUNICATION

## Chiral Self-Discrimination and Guest Recognition in Helicene-based Coordination Cages

Thorben R. Schulte, Julian J. Holstein and Guido H. Clever\*<sup>[a]</sup>

**Abstract:** Chiral, nano-sized confinements play a major role for enantioselective recognition and reaction control in biological systems. Supramolecular self-assembly gives access to artificial mimics with tunable sizes and properties. Here, a new family of [Pd<sub>2</sub>L<sub>4</sub>] coordination cages based on a chiral [6]helicene backbone is introduced. The racemic mixture of bis-monodentate pyridyl ligand **L**<sup>1</sup> assembles with Pd<sup>II</sup> cations under chiral self-discrimination selectively to an achiral *meso* cage *cis*-[Pd<sub>2</sub>L<sup>1P</sup><sub>2</sub>L<sup>1M</sup><sub>2</sub>]. Enantiopure **L**<sup>1</sup> forms homochiral cages [Pd<sub>2</sub>L<sup>1P/M</sup><sub>4</sub>]. Longer derivative **L**<sup>2</sup> forms chiral cages [Pd<sub>2</sub>L<sup>2P/M</sup><sub>4</sub>] with larger cavities, able to bind optical isomers of chiral guests with different affinities. Owing to its distinct chiroptical properties, this cage can distinguish non-chiral guests of different lengths, as they were found to squeeze or elongate the cavity under modulation of the helicenes' helical pitch. CD spectroscopic results are supported by ion mobility mass spectrometry. **L**<sup>2</sup> was further found to yield a unique homochiral, interpenetrated double-cage [Pd<sub>4</sub>L<sup>2P/M</sup><sub>8</sub>], as supported by NMR, MS and single crystal X-ray results.

Nanosized cages based on metallosupramolecular self-assembly have become major players in host-guest chemistry owing to their structural and functional variability and modular composition.<sup>[1]</sup> Recent design-based approaches allow for positioning multiple building blocks by thermodynamically controlled integrative self-sorting.<sup>[2]</sup> In biological host-guest systems, enantioselective recognition takes a pivotal role due to the inherent homochirality of most natural compounds. Hence, the formation of synthetic chiral hosts for enantioselective guest binding is not only of fundamental interest, but provides the basis for the development of selective sensors, transporters and catalysts.<sup>[3]</sup>

Numerous chiral hosts based on covalent macrocyclic molecules such as cyclodextrins, cyclophanes and calixarenes have been reported.<sup>[4]</sup> Chirality has also been reported to facilitate the assembly of hydrogen-bonded organic cages.<sup>[5]</sup> More recently, chiral metallo-supramolecular self-assembled rings and cages have been introduced as selective receptors and enzyme-like nanoreactors based on chiral backbones, auxiliaries, the inherent chirality of stereogenic metal centers or the overall architecture.<sup>[6]</sup> Upon metal coordination, racemic mixtures of ligands may undergo chiral self-sorting,<sup>[7]</sup> leading to homochiral<sup>[8,9,10]</sup> or heterochiral<sup>[10,11]</sup> assemblies. Beyond their use in enantioselective recognition, chiral cages based on luminescent metal centers have been shown to exhibit unique chiroptical properties.<sup>[9,12]</sup> With respect to mechanically interlocked coordination cages,<sup>[13]</sup> reports covering the implementation of homochirality are still scarce, with Hardie's dimer of cyclotriferatrylene-based coordination cages serving as a notable example.<sup>[14]</sup>

Since their discovery in 1912,<sup>[15]</sup> helicenes have been widely studied for properties related to their helical chirality.<sup>[16]</sup> While helicenes have shown appearance in several supramolecular systems, they have never been used in the construction of coordination-driven cages.<sup>[17]</sup> We herein demonstrate, that, despite their highly twisted appearance, helicene-based bis monodentate ligands can be used to assemble discrete [Pd<sub>2</sub>L<sub>4</sub>] coordination cages exhibiting chirality-driven effects on their assembly and guest binding. We further deliver the first example of a homochiral interpenetrated [Pd<sub>4</sub>L<sub>8</sub>] dimer, comprising eight interlocked helicenes.

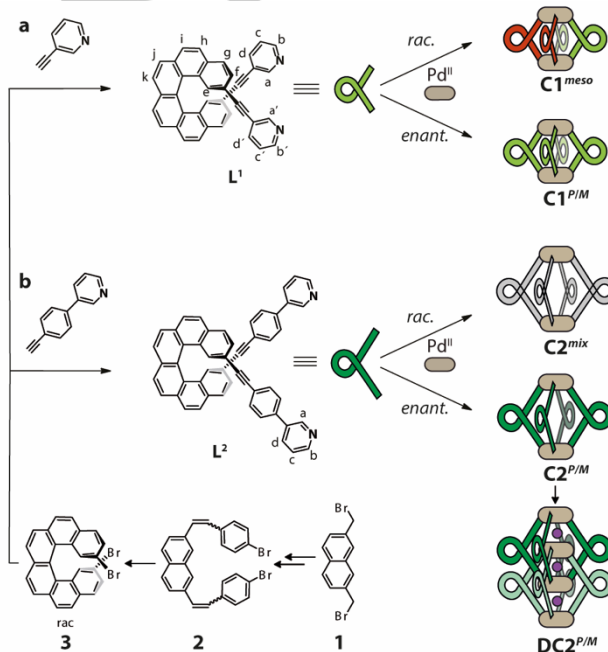


**Figure 1.** a), b) Synthesis of ligands **L**<sup>1</sup> and **L**<sup>2</sup> from 2,15-dibromo[6]helicene **3** followed by separation into the *P* (red color) and *M* (green color) enantiomers. Addition of stoichiometric amounts of Pd<sup>II</sup> leads to quantitative formation of different coordination cages, depending on the ligands' enantiomeric composition and length. Racemic **L**<sup>1</sup> exclusively gives **C1**<sup>meso</sup>, whereas racemic **L**<sup>2</sup> leads to a statistical mixture of all possible stereoisomers (PPPM/MMMP/PPMM/PMPM/PPPP/MMMM, shown in grey color). The enantiopure ligands lead to the chiral coordination cages **C1**<sup>P/M</sup>, **C2**<sup>P/M</sup> and the interpenetrated dimer **DC2**<sup>P/M</sup>.

Ligands **L**<sup>1</sup> and **L**<sup>2</sup> were synthesized via Sonogashira cross coupling reactions from literature-known 2,15-dibromo[6]helicene (Figure 1) to yield racemic products which were separated into the enantiomers by chiral HPLC (SI Figure S23).<sup>[18]</sup> Following our previously reported routines, the bis-monodentate ligands were tested for the formation of self-assembled products using [Pd(CH<sub>3</sub>CN)<sub>4</sub>](BF<sub>4</sub>)<sub>2</sub> as the metal source in different polar organic solvents. Interestingly, in deuterated dmsO the racemic mixture of ligand **L**<sup>1</sup> was found to assemble under chiral self-sorting

[a] Dr. T. R. Schulte, Dr. J. J. Holstein, Prof. Dr. G. H. Clever  
Faculty of Chemistry and Chemical Biology,  
TU Dortmund University, Otto-Hahn-Str. 6, 44227 Dortmund  
(Germany)  
E-mail: guido.clever@tu-dortmund.de

Supporting information for this article is given via a link at the end of the document.

## COMMUNICATION

quantitatively to achiral *meso* cage *cis*-[Pd<sub>2</sub>L<sup>1P</sup>L<sup>1M</sup>]<sub>2</sub> (**C1<sup>meso</sup>**), containing both ligand enantiomers in a 1 : 1 ratio, as confirmed by <sup>1</sup>H (Figure 2a) and NOESY NMR spectroscopy (Figure 4b). For all herein described cages, the <sup>1</sup>H NMR signals of the pyridine moieties (i.e. protons H<sub>a</sub> and H<sub>b</sub>) undergo a downfield shift upon coordination to the palladium(II) cations. The formation of the *meso* cage leads to splitting of all <sup>1</sup>H NMR signals into two sets of equal intensity. All signals could be assigned with the help of 2D NMR techniques (COSY, NOESY, HSQC) indicating that the upper and the lower half of the ligand **L**<sup>1</sup> have ended up in a different surrounding upon cage formation (Supporting Information). The signal splitting can be explained via symmetry considerations. The halves of the *P* helicenes and the halves of *M* helicenes facing each other have the same chemical surrounding resulting in the same chemical shifts for the corresponding protons. Compared to this, one half of the *P* helicene facing the other half of the *P* helicene (same for *M* helicenes) has a different chemical surrounding which explains the twofold splitting in the <sup>1</sup>H NMR spectrum. A tentative *trans*-configured cage would not lead to such a splitting of the NMR signals, since the resulting *D*<sub>2d</sub> symmetry would offer two *C*<sub>2</sub> axes perpendicular to the major *C*<sub>2</sub> axis going through both Pd centers that would allow converting the upper half of each ligand into its lower part (SI Figure S7).

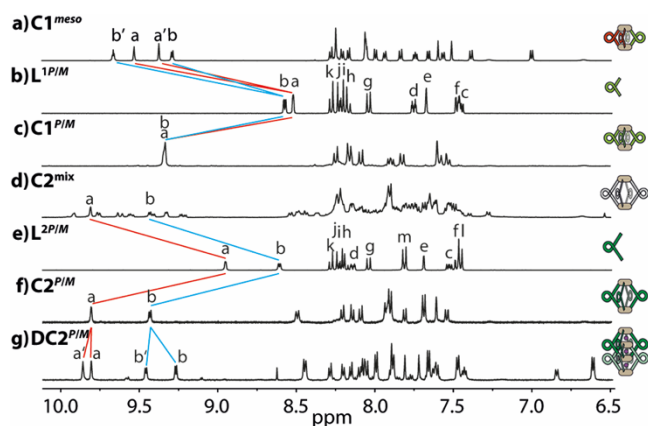


**Figure 2.** <sup>1</sup>H NMR spectra (400 MHz, dms<sub>o</sub>-d<sub>6</sub>, 293 K). a) **C1<sup>meso</sup>**, b) **L<sup>1P/M</sup>**, c) homochiral **C1<sup>P/M</sup>**, d) statistical mixture of **C2** stereoisomers, e) **L<sup>2P/M</sup>**, f) homochiral **C2<sup>P/M</sup>** and g) the homochiral interpenetrated cage structure **DC2<sup>P/M</sup>** (here: 600 MHz, acetonitrile-d<sub>3</sub>, 293 K).

In contrast, the assembly with the enantiopure ligand **L**<sup>1</sup>, either in its *P* or *M* form leads to a homochiral cage with no splitting of the <sup>1</sup>H NMR signals (Figure 2c). In their high resolution ESI mass spectra, cage **C1<sup>meso</sup>** (SI Figure S9) and enantiopure cages **C1<sup>P/M</sup>** (SI Figure S11) could be identified as tetracationic [Pd<sub>2</sub>L<sub>4</sub>]<sup>4+</sup>.

Next, chiral guest discrimination of **C1<sup>P</sup>** was tested with (1*R*) and (1*S*) camphor sulfonate anions **G1<sup>R/S</sup>**, however, no evidence for uptake of the guests was found (SI Figure S21). Most probable reason is the limited size of the cavity, known as a critical factor for guest binding.<sup>[19]</sup> To permit guest encapsulation, the ligand structure was extended by including 1,4-phenylene linkers on both sides to give ligand **L**<sup>2</sup>. The elongation of the ligands nearly doubles the Pd–Pd distance in the modelled structures (DFT

ωB97XD/def2SVP, PCM solvent: dms<sub>o</sub>) of **C2<sup>P/M</sup>** (20.1 Å) (Figure 4d) compared to **C1<sup>P/M</sup>** (10.4 Å) (Figure 4c). In case of racemic **L**<sup>2</sup>, cage formation leads to splitting of all <sup>1</sup>H NMR signals into several sets, indicative for a lack of chiral self-sorting under formation of a statistical mixture of isomeric species (Figure 2d). This picture is supported by the clean appearance of the high-resolution ESI mass spectrum of this mixture showing only peaks assignable to the tetracationic [Pd<sub>2</sub>L<sub>4</sub>]<sup>4+</sup> species, superimposable with the spectrum of the homochiral cage **C2<sup>P/M</sup>** (SI Figure S14). The absence of chiral self-discrimination encountered upon cage formation from racemic **L**<sup>2</sup> can be explained with the increased distance between the helicene backbones (based on calculated structures of cages **C1** and **C2**, the closest H–H distance between two neighboring backbones has increased from 2.39 Å to 6.20 Å).

In contrast to the results obtained in dms<sub>o</sub>, heating the enantiopure ligand **L**<sup>2</sup> with palladium(II) cations in acetonitrile was found to lead to a splitting of all NMR signals into two sets of equal intensity, thus indicating the formation of a chiral interpenetrated cage **DC2<sup>P/M</sup>** (Figure 2g).<sup>[13]</sup> In addition, the high-resolution ESI mass spectrum revealed signals for the dimeric species [3BF<sub>4</sub>@Pd<sub>4</sub>L<sub>8</sub>]<sup>5+</sup> (Figure 3c).

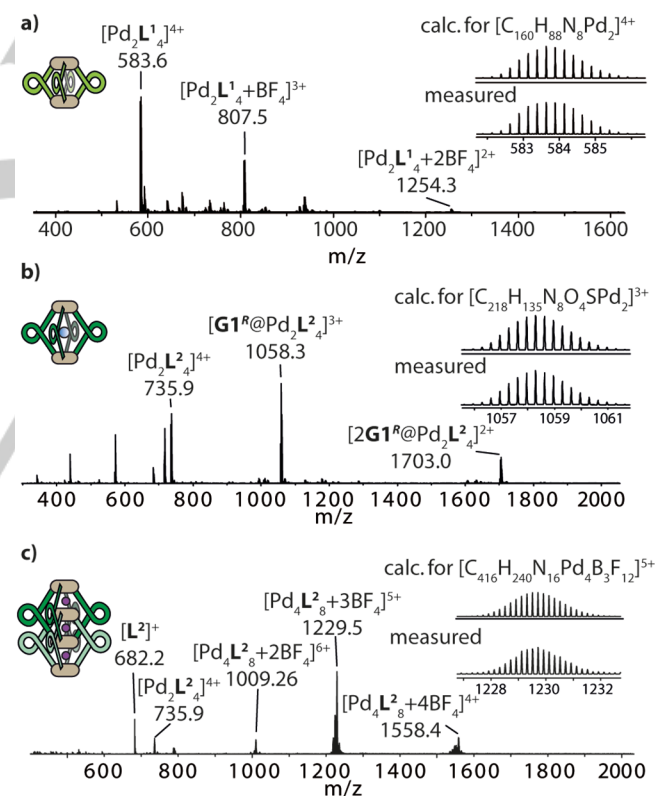


**Figure 3.** ESI mass spectra of a) cage **C1<sup>M</sup>**, b) cage **C2<sup>M</sup>** after addition of (1*R*)-camphor sulfonate **G1<sup>R</sup>**, c) double cage **DC2<sup>M</sup>**.

Further structural insight was delivered by X-ray diffraction methods. Crystals of enantiopure **L**<sup>2</sup> (second HPLC fraction eluted from a Chiralpak IC column) suitable for X-ray structure analysis could be obtained by crystallization from dms<sub>o</sub> (Figure 4e). The asymmetric unit contained twelve individual helicene ligands, all of which are highly intertwined in a remarkably

## COMMUNICATION

unordered fashion (SI Figure S25). The absolute configuration was unambiguously determined as the (*P*) enantiomer using the method of Parsons<sup>[20]</sup> as implemented in SHELXL,<sup>[21]</sup> yielding an enantiopurity distinguishing parameter of  $x = 0.079(8)$ . This assignment is in agreement with measured circular dichroism (CD) spectra of this compound as compared to published data on similarly substituted [6]helicenes and DFT-calculated CD bands.<sup>[22,23]</sup>

Single crystals of the dimeric cage species [2PF<sub>6</sub><sup>-</sup>@Pd<sub>4</sub>L<sup>2M</sup>]<sub>2</sub> (**DC2<sup>M</sup>**), based on the *M* ligand enantiomer eluting first from the chiral column), suitable for X-ray structure analysis were obtained by slow diffusion of diethyl ether into an acetonitrile solution of the cage containing PF<sub>6</sub><sup>-</sup> counter anions (Figure 4f). Synchrotron radiation was required for obtaining diffraction data that could be solved with direct methods using SHELXT.<sup>[24]</sup> Again, the absolute configuration could be unambiguously determined, yielding an enantiopurity distinguishing parameter of  $x = -0.02(2)$ . CD data was found to be in agreement with the literature reported absolute structure assignment of comparable helicenes.<sup>[22,23]</sup> The structure reveals that the double cage features three consecutive pockets, the two outer ones filled with a PF<sub>6</sub><sup>-</sup> anion. The Pd–Pd distances are 8.66 Å for the outer pockets and 10.33 Å for the inner cavity.

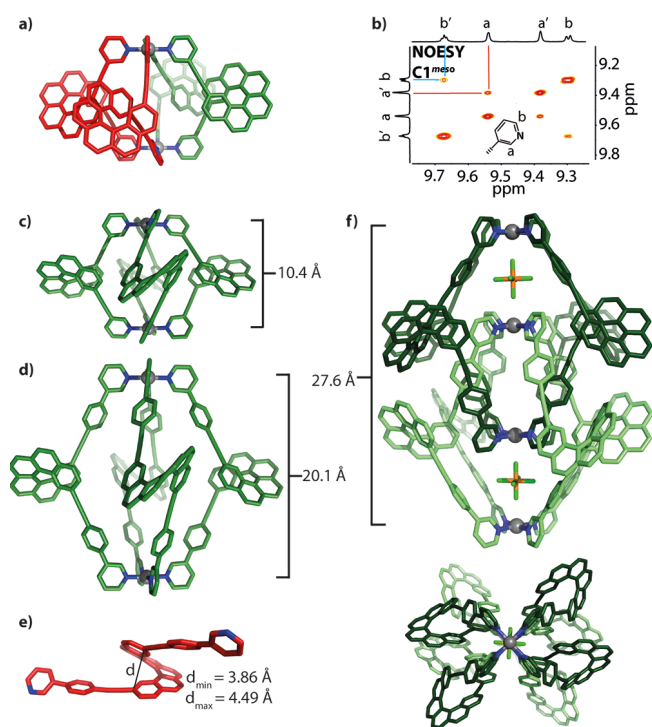


**Figure 4.** a) DFT-calculated structure of **C1<sup>meso</sup>**, b) NOESY NMR detail of the **C1<sup>meso</sup>** cage supporting the *cis* ligand arrangement, c) and d) calculated structures of **C1<sup>M</sup>** and **C2<sup>M</sup>**. e) One of twelve **L<sup>2P</sup>** molecules in the asymmetric unit of its solid state structure with found min/max. helical pitches. f) X-ray crystal structure of **DC2<sup>M</sup>**, side and top view along the Pd<sub>4</sub> axis (Pd: grey, N: blue, C: green (*M* enantiomer), red (*P* enantiomer), P: orange, F: light green).

Having the large cavity of monomeric **C2<sup>P/M</sup>** in hand, chiral guest discrimination could be shown for the enantiopure cages via <sup>1</sup>H NMR titration experiments by stepwise addition of camphor sulfonates **G1<sup>R</sup>** and **G1<sup>S</sup>** as their tetrabutyl ammonium salts. Characteristic downfield shifts for the inside-pointing proton H<sub>a</sub>

were observed (SI Figure 22) and the results are summarized as a comparison of binding isotherms ( $\Delta\delta$  plot; Figure 5c). Pleasingly, both guest enantiomers showed different binding behavior when exposed to the same chiral cage, however, the combination **G1<sup>S</sup>@C2<sup>P</sup>** showed the same behavior as the enantiomeric system **G1<sup>R</sup>@C2<sup>M</sup>**, with binding constants of around 560 M<sup>-1</sup>.<sup>[25]</sup> The diastereomeric combinations to this, **G1<sup>R</sup>@C2<sup>P</sup>** and **G1<sup>S</sup>@C2<sup>M</sup>**, showed a stronger extent of NMR signal shifting and a binding constant of around 1010 M<sup>-1</sup>. In the high resolution ESI mass spectra, the host-guest complexes could be identified as the triple cationic species [**G1**@Pd<sub>2</sub>L<sup>2</sup>]<sub>3</sub><sup>3+</sup> (Figure 3b).

Furthermore, CD spectra were compared for **L<sup>1P/M</sup>** and **C1<sup>P/M</sup>** (SI Figure S24) and **L<sup>2P/M</sup>** and **C2<sup>P/M</sup>** (Figure 5a), showing a strong circular dichroism for the ligands and the cages with a positive Cotton effect for the (*P*) enantiomers. We next set out to investigate the potential utilization of the strong CD effect as an indicator for the discrimination of achiral guests. Since the cages consist of four helicenes arranged like parallel springs around two connecting Pd(II) cations, we envisioned that charged guests encapsulated between these electrostatic anchors should modulate the helical pitch of the ligand backbones. First, we compared the effect of binding short 2,7-naphthalene disulfonate **G2** and long 4,4'-biphenyl disulfonate **G3** on the CD spectra of **C2<sup>P</sup>**. Difference spectra revealed that encapsulation of the shorter guest leads to a decrease of CD band intensity around 360 nm while binding of the longer guest increases intensity of the same band (Figure 5b). The assumption that such an effect is caused by tuning the helicenes' helical pitch was predicted by theoretical work of Mori and Inoue *et al.*<sup>[22]</sup> We were able to confirm this hypothesis by calculating the relative CD signal intensities of unsubstituted [6]helicene under variation of its helical pitch within the limits found in the twelve individual ligands contained in the solid state structure of **L<sup>2</sup>** (SI Figure S26 and Figure 4e).

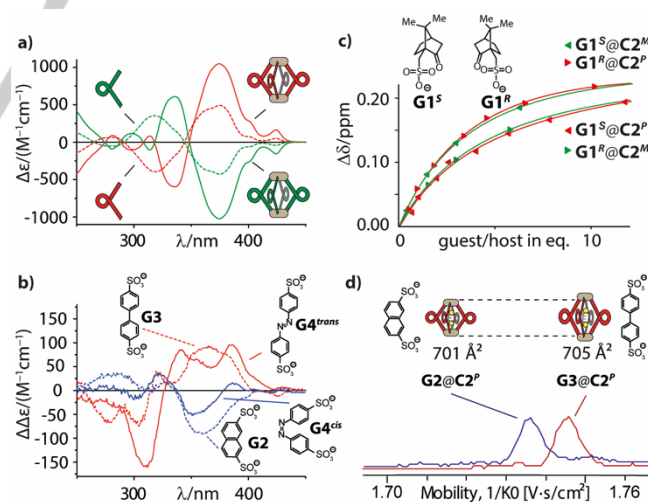


**Figure 5.** a) Circular dichroism spectra of ligands **L<sup>2P/M</sup>** and cages **C2<sup>P/M</sup>** and b) difference CD spectra (free host CD subtracted from host-guest CD) of **G2@C2<sup>P</sup>** and **G3@C2<sup>P</sup>** as well as **G4<sup>trans</sup>@C2<sup>P</sup>** and **G4<sup>cis</sup>@C2<sup>P</sup>** (all in dmso). c) Comparison of binding isotherms for all four diastereomeric host-guest combinations **G1<sup>RS</sup>@C2<sup>P/M</sup>** showing two 'matched' and two 'mismatched' cases; d) Superposition of mobilograms obtained by trapped ion mobility ESI-TOF mass spectrometry for host-guest complexes **G2@C2<sup>P</sup>** (mobility 1/K<sub>0</sub>: 1.736 Vs/cm<sup>2</sup>, CCS: 701 Å<sup>2</sup> at *m/z* 1615.4) and **G3@C2<sup>P</sup>** (mobility 1/K<sub>0</sub>: 1.745 Vs/cm<sup>2</sup>, CCS: 705 Å<sup>2</sup> at *m/z* 1627.9).

## COMMUNICATION

Further, direct evidence for a shrinking and expansion of the cages upon addition of the short and long guest, respectively, came from trapped ion mobility ESI-TOF mass spectrometry (timsTOF), which indicates a smaller gas phase collisional cross section for **G2@C2<sup>P</sup>** (701 Å<sup>2</sup>) than for **G3@C2<sup>P</sup>** (705 Å<sup>2</sup>), even in a mixture of both host-guest complexes (Figure 5d and SI Figure S27).<sup>[26]</sup> We repeated the CD experiment with azobenzene-based guest **G4**,<sup>[27]</sup> either in its *cis* or *trans* photoisomeric form (Figure 5b). Remarkably, the effect of band intensity decrease/increase could be reproduced and allows the differentiation between the *cis* and the *trans* form of achiral azobenzene via CD spectroscopy, keeping in mind that the free guest itself shows no CD effect. In addition, observed deviations from the expected band shapes were attributed to a certain degree of chirality transfer on the azobenzene chromophore which – in contrast to guests **G2** and **G3** – shows significant absorption around 360 nm.

In summary, a new family of [Pd<sub>2</sub>L<sub>4</sub>] coordination cages based on a chiral helicene backbone has been developed.<sup>[28]</sup> One of the cages showed integrative chiral self-sorting, thus serving as an example for the non-statistical formation of heteroleptic structures, while another was found to discriminate chiral guests via differing binding affinities to its enantiopure form. The strong circular dichroism of the helicene backbone could further be exploited for the size discrimination of achiral anionic guests by taking advantage of modulating the system's chiroptical properties upon guest-induced changes of the helical pitch. Ion mobility mass spectrometry was employed to support these findings. In addition, the group of [Pd<sub>4</sub>L<sub>8</sub>] interpenetrated cages could be expanded by an unprecedented chiral species, illustrated by its single crystal X-ray structure. Further studies are underway to expand the guest binding and recognition features and develop a system for enantioselective catalysis inside confined environments.

## Experimental Section

Cages **C1** and **C2** were formed by addition of [Pd(CH<sub>3</sub>CN)<sub>4</sub>](BF<sub>4</sub>)<sub>2</sub> (0.5 eq.) to the corresponding ligands (racemic or enantiopure) in dmsO at 23 °C. Cage **DC2** was formed after heating **C2** in MeCN at 75 °C for 2 weeks. Single crystals suitable for X-ray structure determination were grown for **L<sup>2P</sup>** from dmsO and for **DC2<sup>M</sup>** by slow diffusion of Et<sub>2</sub>O into a **L<sup>2M</sup>** plus [Pd(CH<sub>3</sub>CN)<sub>4</sub>](PF<sub>6</sub>)<sub>2</sub> mixture in MeCN at 7 °C. CCDC 1558206 (**L<sup>2P</sup>**) and CCDC 1581540 (**DC2<sup>M</sup>**) contain the supplementary crystallographic data for this paper. These data can be obtained free of charge from The Cambridge Crystallographic Data Centre via [www.ccdc.cam.ac.uk/data\\_request/cif](http://www.ccdc.cam.ac.uk/data_request/cif).

## Acknowledgements

This work has been supported by the Deutsche Forschungsgemeinschaft (CL 489/2-2, RESOLV Cluster of Excellence EXC-2033 – project number 390677874) and the European Research Council through ERC Consolidator grant 683083 (RAMSES). We thank Prof. U. Diederichsen, Prof. L. Ackermann and Prof. L. Tietze (all Georg-August University Göttingen) for access to CD and HPLC facilities. We further thank S. Löffler for support with

crystallization experiments, Prof. W. Hiller (TU Do), Dr. M. John (GAU Gö) for help with NMR spectroscopy and L. Schneider (TU Do), C. Heitbrink, Dr. P. Janning (MPI Do) and Dr. H. Frauendorf (GAU Gö) for ESI mass spectra. Diffraction data for **DC2<sup>M</sup>** was collected at PETRA III, DESY a member of the Helmholtz Association (HGF). The authors thank Saravanan Panneerselvam for assistance in using synchrotron beamline P11, (I-20160736).<sup>[29]</sup>

**Keywords:** chirality • anion recognition • host-guest chemistry • interpenetration • supramolecular chemistry

- [1] a) R. Chakrabarty, P. S. Mukherjee, P. J. Stang, *Chem. Rev.* **2011**, *111*, 6810; b) M. Han, D. M. Engelhard, G. H. Clever, *Chem. Soc. Rev.* **2014**, *43*, 1848.
- [2] a) S. Mukherjee, P. S. Mukherjee, *Chem. Commun.* **2014**, *50*, 2239; b) W. M. Bloch, G. H. Clever, *Chem. Commun.* **2017**, *53*, 8506.
- [3] a) A. M. Castilla, W. J. Ramsay, J. R. Nitschke, *Acc. Chem. Res.* **2014**, *47*, 2063; b) L.-J. Chen, H.-B. Yang, M. Shionoya, *Chem. Soc. Rev.* **2017**, *46*, 2555; c) M. Pan, K. Wu, J.-H. Zhang, C.-Y. Su, *Coord. Chem. Rev.* **2019**, *378*, 333.
- [4] a) Y. Tsunoda, K. Fukuta, T. Imamura, R. Sekiya, T. Furuyama, N. Kobayashi, T. Haino, *Angew. Chem. Int. Ed.* **2014**, *53*, 7243; b) C. Gropp, N. Trapp, F. Diederich, *Angew. Chem. Int. Ed.* **2016**, *55*, 14444.
- [5] D. Beaudoin, F. Rominger, M. Mastalerz, *Angew. Chem. Int. Ed.* **2016**, *55*, 15599.
- [6] a) C. J. Carrano, K. N. Raymond, *J. Am. Chem. Soc.* **1978**, *100*, 5371; b) S. J. Lee, W. Lin, *J. Am. Chem. Soc.* **2002**, *124*, 4554; c) G. A. Hembury, V. V. Borovkov, Y. Inoue, *Chem. Rev.* **2008**, *108*, 1; d) Y. Nishioka, T. Yamaguchi, M. Kawano, M. Fujita, *J. Am. Chem. Soc.* **2008**, *130*, 8160; e) C. Siering, J. Toräng, H. Kruse, S. Grimme, S. R. Waldvogel, *Chem. Commun.* **2010**, *46*, 1625; f) C. Zhao, Q.-F. Sun, W. M. Hart-Cooper, A. G. DiPasquale, F. D. Toste, R. G. Bergman, K. N. Raymond, *J. Am. Chem. Soc.* **2013**, *135*, 18802; g) C. Gütz, R. Hovorka, C. Klein, Q.-Q. Jiang, C. Bannwarth, M. Engeser, C. Schmuck, W. Assenmacher, W. Mader, F. Topić et al., *Angew. Chem. Int. Ed.* **2014**, *53*, 1693.
- [7] H. Jędrzejewska, A. Szumna, *Chem. Rev.* **2017**, *117*, 4863.
- [8] a) M. A. Masood, E. J. Enemark, T. D. P. Stack, *Angew. Chem. Int. Ed.* **1998**, *37*, 928; b) A. Lützen, M. Hapke, J. Griep-Raming, D. Haase, W. Saak, *Angew. Chem. Int. Ed.* **2002**, *41*, 2086; c) U. Kiehne, T. Weilandt, A. Lützen, *Org. Lett.* **2007**, *9*, 1283; d) C. Maeda, T. Kamada, N. Aratani, A. Osuka, *Coord. Chem. Rev.* **2007**, *251*, 274; e) G. Meyer-Eppler, F. Topić, G. Schnakenburg, K. Rissanen, A. Lützen, *Eur. J. Inorg. Chem.* **2014**, *2014*, 2495; f) S. A. Boer, D. R. Turner, *Chem. Commun.* **2015**, *51*, 17375; g) L.-L. Yan, C.-H. Tan, G.-L. Zhang, L.-P. Zhou, J.-C. Bünzli, Q.-F. Sun, *J. Am. Chem. Soc.* **2015**, *137*, 8550; h) V. E. Pritchard, D. Rota Martir, S. Oldknow, S. Kai, S. Hiraoka, N. J. Cookson, E. Zysman-Colman, M. J. Hardie, *Chemistry* **2017**, *23*, 6290; i) T. Tateishi, T. Kojima, S. Hiraoka, *Commun Chem* **2018**, *1*, 727.
- [9] L.-L. Yan, C.-H. Tan, G.-L. Zhang, L.-P. Zhou, J.-C. Bünzli, Q.-F. Sun, *J. Am. Chem. Soc.* **2015**, *137*, 8550.
- [10] D. Beaudoin, F. Rominger, M. Mastalerz, *Angew. Chem. Int. Ed.* **2017**, *56*, 1244.
- [11] a) T. W. Kim, J.-I. Hong, M. S. Lah, *Chem. Commun.* **2001**, 743; b) C. G. Claessens, T. Torres, *J. Am. Chem. Soc.* **2002**, *124*, 14522; c) T. Weilandt, U. Kiehne, G. Schnakenburg, A. Lützen, *Chem. Commun.* **2009**, 2320; d) C. S. Arribas, O. F. Wendt, A. P. Sundin, C.-J. Carling, R. Wang, R. P. Lemieux, K. Wärnmark, *Chem. Commun.* **2010**, *46*, 4381.
- [12] a) D. Rota Martir, D. Escudero, D. Jacquemin, D. B. Cordes, A. M. Z. Slawin, H. A. Fruchtl, S. L. Warriner, E. Zysman-Colman, *Chem. Eur. J.* **2017**, *23*, 14358; b) X.-Z. Li, L.-P. Zhou, L.-L. Yan, D.-Q. Yuan, C.-S. Lin, Q.-F. Sun, *J. Am. Chem. Soc.* **2017**, *139*, 8237.
- [13] M. Frank, M. D. Johnstone, G. H. Clever, *Chem. Eur. J.* **2016**, *22*, 14104.
- [14] A. Westcott, J. Fisher, L. P. Harding, P. Rizkallah, M. J. Hardie, *J. Am. Chem. Soc.* **2008**, *130*, 2950.
- [15] R. Weitzenböck, H. Lieb, *Monatsh. Chem.* **1912**, *33*, 549.
- [16] a) M. Gingras, *Chem. Soc. Rev.* **2013**, *42*, 968; b) N. Saleh, C. Shen, J. Crassous, *Chem. Sci.* **2014**, *5*, 3680; c) C.-F. Chen, Y. Shen, *Helicene Chemistry*, Springer, Berlin, Heidelberg, **2017**; d) K. Mori, T. Murase, M. Fujita, *Angew. Chem. Int. Ed.* **2015**, *54*, 6847; e) J. R. Brandt, X. Wang, Y. Yang, A. J. Campbell, M. J. Fuchter, *J. Am. Chem. Soc.* **2016**, *138*, 9743.
- [17] a) T. Verbiest, S. Van Elshocht, M. Kauranen, L. Hellemans, J. Snauwaert, C. Nuckolls, T. J. Katz, A. Persoons, *Science* **1998**, *282*, 913; b) T. Kaseyama, S. Furumi, X. Zhang, K. Tanaka, M. Takeuchi, *Angew. Chem.* **2011**, *123*, 3768.
- [18] a) A. Terfort, H. Görls, H. Brunner, *Synthesis* **1997**, *1997*, 79; b) J. M. Fox, D. Lin, Y. Itagaki, T. Fujita, *J. Org. Chem.* **1998**, *63*, 2031.

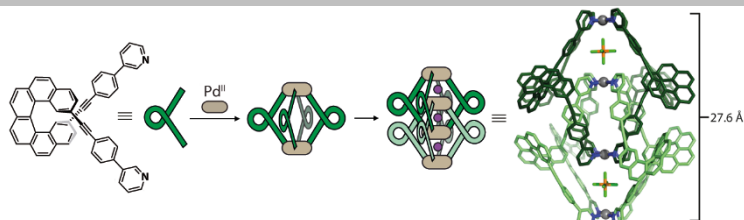
## COMMUNICATION

- [19] a) S. Löffler, J. Lübber, A. Wuttke, R. A. Mata, M. John, B. Dittrich, G. H. Clever, *Chem. Sci.* **2016**, *7*, 4676; b) S. Freye, R. Michel, D. Stalke, M. Pawliczek, H. Frauendorf, G. H. Clever, *J. Am. Chem. Soc.* **2013**, *135*, 8476.
- [20] S. Parsons, H. D. Flack, T. Wagner, *Acta Cryst. B* **2013**, *69*, 249.
- [21] G. M. Sheldrick, *Acta Cryst. C* **2015**, *71*, 3.
- [22] Y. Nakai, T. Mori, Y. Inoue, *J. Phys. Chem. A* **2012**, *116*, 7372.
- [23] Y. Nakai, T. Mori, Y. Inoue, *J. Phys. Chem. A* **2013**, *117*, 83.
- [24] G. M. Sheldrick, *Acta Cryst. A* **2015**, *71*, 3.
- [25] P. Thordarson, *Chem. Soc. Rev.* **2011**, *40*, 1305.
- [26] a) O. Jurček, P. Bonakdarzadeh, E. Kalenius, J. M. Linnanto, M. Groessel, R. Knochenmuss, J. A. Ihalainen, K. Rissanen, *Angew. Chem. Int. Ed.* **2015**, *54*, 15462; b) J.-F. Greisch, J. Chmela, M. E. Harding, D. Wunderlich, B. Schäfer, M. Ruben, W. Klopfer, D. Schooss, M. M. Kappes, *Phys. Chem. Chem. Phys.* **2017**, *19*, 6105.
- [27] G. H. Clever, S. Tashiro, M. Shionoya, *J. Am. Chem. Soc.* **2010**, *132*, 9973.
- [28] a) A. U. Malik, F. Gan, C. Shen, N. Yu, R. Wang, J. Crassous, M. Shu, H. Qiu, *J. Am. Chem. Soc.* **2018**, *140*, 2769; b) T. Matsushima, S. Kikkawa, I. Azumaya, S. Watanabe, *ChemistryOpen* **2018**, *7*, 278.
- [29] A. Burkhardt, T. Pakendorf, B. Reime, J. Meyer, P. Fischer, N. Stübe, S. Panneerselvam, O. Lorbeer, K. Stachnik, M. Warmer P. Rödiger, D. Görjes, A. Meents, *Eur. Phys. J. Plus* **2016**, *131*, 56.

## COMMUNICATION

## Entry for the Table of Contents

## COMMUNICATION



Thorben R. Schulte, Julian J. Holstein  
and Guido H. Clever\*

Page No. – Page No.

**Chiral Self-Discrimination and Guest  
Recognition in Helicene-based  
Coordination Cages**

Chiral [6]helicenes serve as building blocks for the assembly of [Pd<sub>2</sub>L<sub>4</sub>] coordination cages and interpenetrated [Pd<sub>4</sub>L<sub>8</sub>] dimers. Depending on the ligand length, chiral self-discrimination and recognition of enantiomeric guests is observed. Helical pitch modulation allows the discrimination of non-chiral guests by a combination of CD spectroscopy and ion mobility mass spectrometry.